Band structures of II-VI semiconductors using Gaussian basis functions with separable *ab initio* pseudopotentials: Application to prediction of band offsets

Xiaojie Chen, Xinlei Hua, Jinsong Hu, Jean-Marc Langlois,* and William A. Goddard III†
Materials and Molecular Simulation Center, Beckman Institute (139-74), Division of Chemistry and Chemical Engineering (CN9043), California Institute of Technology, Pasadena, California 91125
(Received 17 February 1995)

We describe the implementation of a separable pseudopotential into the dual space approach for *ab initio* density-functional calculations using Gaussian basis functions. We apply this Gaussian dual space method (GDS/DFT) to the study of II-VI semiconductors (II=Zn, Cd, Hg; VI=S, Se, Te, Po). The results compare well with experimental data and demonstrate the general transferability of the separable pseudopotential. We also introduce a band-consistent tight-binding (BC-TB) model for calculating the bulk contributions to the valence-band offsets (VBO's). This BC-TB approach yields good agreement with all-electron *ab initio* GDS/DFT results. Comparisons between BC-TB results of VBO obtained with and without p-d coupling demonstrate quantitatively the importance of d electrons and cation-d–anion-p coupling in II-VI systems. Agreement between *ab initio* results and experimental results is excellent.

I. INTRODUCTION

We have recently developed the dual space approach for using Gaussian basis functions[1] in first-principles density-functional calculations of the electronic band structures of crystals. This method (GDS/DFT) has previously been applied to all-electron calculations of crystals (two and three dimensions), leading to results in good agreement with plane-wave calculations and with experiment. Here we extend the method for applications using pseudopotentials (referred to as GDSP/DFT). Using pseudopotentials from *ab initio* relativistic atomic calculations, one can take into account the scalar relativistic effects for heavy atoms while using the nonrelativistic Kohn-Sham equations for the valence electrons. The use of pseudopotentials (PP) significantly reduces numerical errors since the energy spectra width is greatly reduced (due to the frozen core).

For the specific applications, we use the Bachelet-Hamann-Schlüter[2] (BHS) PP but in the separable form (PP/S) we recently developed.[3] The nonlocal BHS PP has been widely applied to calculations using plane-wave basis sets, allowing direct comparisons with the Gaussian-based studies and with the separable PP of previous theoretical calculations. The separable PP maintains the general transferability[1] of the nonlocal BHS PP while decreasing computational costs to construct the PP matrix elements over Gaussian basis functions. This leads to linear scaling of the cost with basis set size whereas the cost of using the nonlocal BHS form scales quadratically.

We report here calculations for twelve II-VI semiconductors. The objectives are (1) to demonstrate the accuracy of GDSP/DFT; (2) to extend the applications of the PP/S to more general cases; (3) to provide an electronic structure database for II-VI semiconductors for further studies in superlattices and surfaces of these materials; and (4) to assess quantitatively the importance of d electrons and cation-d–anion-p coupling in II-VI systems.

This paper is organized as follows. In Sec. II, we present the methodology for total-energy calculations using the PP/S approximation. In Sec. III we present results for II-VI semiconductors and compare with experimental data and other theoretical calculations. Section IV contains concluding remarks.

II. TOTAL-ENERGY CALCULATIONS

Using PP to replace the core electrons of various nuclei, the ground-state total energy is written as

$$E_{\rm tot}=E_{\rm kin}+E_{\rm xc}+E_{\rm elect}, \tag{1a}$$

$$E_{\rm elect}=E_{ee}+E_{en}+E_{nn}, \tag{1b}$$

where $E_{\rm kin}$ is the kinetic energy of valence electrons, $E_{\rm xc}$ is the electronic exchange-correlation energy of valence electrons, E_{ee} is the Coulomb interaction energy between valence electrons, E_{en} contains all interactions between valence electrons and nuclei interactions (modeled by PP), and E_{nn} contains all the nuclei-nuclei interactions (including any residual interactions between the PP).

The calculation of $E_{\rm kin}$ is done analytically using the Obara and Saika[4] recursion relation. $E_{\rm xc}$ is calculated easily using the numerical grid.[1] The $E_{\rm elect}$ terms take more care.

We use the BHS PP to describe the electron-nuclei interaction. For any center a the BHS PP has the form

$$V_{pp}=V^{\rm loc}_{pp,a}+V^{\rm nl}_{pp,a}, \tag{2a}$$

where $V^{\rm nl}_{pp,a}$ contains angular momentum projection operators with respect to center a making it nonlocal. Here $V^{\rm loc}_{pp,a}$ is a simple function of distance (a local potential). However, the terms in $V^{\rm nl}_{pp,a}$ decrease exponentially with distance (r) whereas $V^{\rm loc}_{pp,a}$ has the form $-Za/r$ for large r. The long-range part of V_{pp} can be written as

$$V^{\rm loc}_{pp,a}(\mathbf{r})=-\frac{Z_a}{r}\sum_{i=1}^{2} C_i\ {\rm erf}(\sqrt{\alpha_i}r), \tag{2b}$$

where Z_a is the number of (explicit) valence electrons, e.g., 4 for Si (the PP parameters C_i and α_i were obtained from atomic calculations by BHS). The nonlocal term has the form

$$V_{pp,a}^{\rm nl}(\mathbf{r}) = \sum_{lm} |lm\rangle U_{la}(r)\langle lm|, \tag{2c}$$

where the $\langle lm|$ are spherical harmonic projection operators and the $U_{la}(r)$ have no long-range tails (they go to zero exponentially). In the applications reported here, we use the BHS PP as tabulated in Ref. 2 for $U_{la}(r)$. Summing $V_{pp,a}^{\rm loc}$ over all atoms of the crystal leads to the Coulomb potential

$$V_{pp}^{\rm loc} = \sum_a V_{pp,a}^{\rm loc}. \tag{3a}$$

Solving the Poisson equation for (3a) leads then to the pp charge distribution

$$\rho_{pp}(\mathbf{r}) = -\sum_R \sum_a Z_a \sum_{i=1}^{2} C_i \left(\frac{\alpha_i}{\pi}\right)^{3/2} e^{-\alpha_i|\mathbf{r}-\mathbf{R}-\mathbf{a}|^2}, \tag{3b}$$

which corresponds to a sum of Gaussian charge distributions. Here Σ_R runs over unit cells and Σ_a runs over atoms in the unit cell. Thus, considering only $V_{pp}^{\rm loc}$ for the moment leads to

$$E_{en}^{\rm loc} = \int d\mathbf{r}\ \rho_e(\mathbf{r}) V_{pp}^{\rm loc}(\mathbf{r}) = \int d\mathbf{r}_1\ d\mathbf{r}_2\ \frac{\rho_e(\mathbf{r}_1)\rho_{pp}(\mathbf{r}_2)}{|\mathbf{r}_1-\mathbf{r}_2|} \equiv [\rho_e \| \rho_{pp}], \tag{4}$$

where ρ_e is the density of valence electrons.

In terms of ρ_e, E_{ee} becomes

$$E_{ee} = \tfrac{1}{2}[\rho_e \| \rho_e]. \tag{5}$$

Similarly defining

$$\rho_{\rm ion}(\mathbf{r}) = \sum_R \sum_a Z_a \delta(\mathbf{r}-\mathbf{R}-\mathbf{a}), \tag{6a}$$

leads to

$$E_{nn} = \tfrac{1}{2}[\rho_{\rm ion} \| \rho_{\rm ion}], \tag{6b}$$

where it is understood that self-interactions are excluded from E_{nn}.

For an infinite system, E_{en}, E_{nn}, and E_{ee} must be handled carefully because of the long-range nature of the Coulomb interactions. The key point is to calculate electrostatic energies as sums of contributions from neutral charge distributions. As in GDS/DFT,[1] we screen the nuclei and the electrons separately with Gaussian functions.

Using Eqs. (4), (5), and (6) in (1b), the total electrostatic energy becomes

$$E_{\rm elect} = E_{en}^{\rm nl} + E_{\rm Coul}, \tag{7a}$$

where

$$E_{\rm Coul} = E_{ee} + E_{nn} + E_{en}^{\rm loc} \tag{7b}$$

$$= E_{\rm Coul}^{\rm lat} + E_{\rm Coul}^{\rm ele}. \tag{7c}$$

Here

$$E_{\rm Coul}^{\rm lat} = \tfrac{1}{2}[\rho_{\rm ion} \| (\rho_{\rm ion} - \rho_{si})] + \tfrac{1}{2}([\rho_{\rm ion} \| \rho_{si}] - [\rho_{se} \| \rho_{se}]), \tag{8}$$

and

$$E_{\rm Coul}^{ele} = \tfrac{1}{2}[(\rho_e + \rho_{se}) \| (\rho_e + \rho_{se})] + [\rho_e \| (\rho_{pp} - \rho_{se})]. \tag{9}$$

The screening charge ρ_{si} of the ions is given by

$$\rho_{si}(\mathbf{r}) = \sum_R \sum_a Z_a \left(\frac{S_i}{\pi}\right)^{3/2} e^{-s_i|\mathbf{r}-\mathbf{a}-\mathbf{R}|^2}, \tag{10}$$

and the screening charge ρ_{se} of the electrons is given by

$$\rho_{se}(\mathbf{r}) = \sum_R \sum_a Z_a \left(\frac{S_e}{\pi}\right)^{3/2} e^{-s_e|\mathbf{r}-\mathbf{a}-\mathbf{R}|^2}. \tag{11}$$

It is convenient to choose $s_e = 2s_i$ so that the second term in (8) is zero. In this case

$$E_{\rm Coul}^{\rm lat} = \frac{1}{2} \sum_a \sum_b \sum_{R \ni a-b-R \neq 0} \frac{Z_a Z_b}{|\mathbf{a}-\mathbf{b}-\mathbf{R}|} \times \mathrm{erfc}[\sqrt{s_i}|\mathbf{a}-\mathbf{b}-\mathbf{R}|] - \sum_a Z_a^2 \left(\frac{s_i}{\pi}\right)^{1/2}. \tag{12}$$

The calculation of the first term in (9),

$$E_{\rm atm} = \tfrac{1}{2}[(\rho_e + \rho_{se}) \| (\rho_e + \rho_{se})], \tag{13}$$

is done as in GDS/DFT.[1] Thus defining

$$\rho_{\rm atm} \equiv \rho_{se} + \rho_e$$

we see that the integral of $\rho_{\rm atm}$ is zero. We then project $\rho_{\rm atm}$ (using the generalized Becke projection function P_{aR} defined in Ref. 1) into atomic contributions

$$\rho_{\rm atm}(\mathbf{r}) = \sum_R \sum_a P_{aR}(\mathbf{r}) \rho_{\rm atm}(\mathbf{r}) = \sum_R \sum_a \rho_a(\mathbf{r}). \tag{14}$$

Each projected atomic charge ρ_a is then screened and the Coulomb potential from the resulting charge is calculated solving the Poisson equation on the radial grid. The total Coulomb potential due to the valence electron

$$V_e(\mathbf{r}) \equiv \int d\mathbf{r}_1\ \frac{\rho_{\rm atm}(\mathbf{r}_1)}{|\mathbf{r}-\mathbf{r}_1|}$$

is then obtained as a linear superposition of atomic contributions in real space. As in Ref. 1 any numerical errors $\delta\rho$, resulting from the projection in (14) are corrected by transforming $\delta\rho$ into reciprocal space.[1] Given V_e, $E_{\rm atm}$ is calculated using numerical integration

$$E_{\rm atm} = \int d\mathbf{r}\ V_e(\mathbf{r}) \rho_{\rm atm}(\mathbf{r}).$$

The second term of (9), the interaction of the electron density with the difference between ρ_{pp} and ρ_{se},

$$E_{e,pp} \equiv [\rho_e \| (\rho_{pp} - \rho_{se})]$$

is calculated by first constructing analytically the potential from the neutral charge distribution

TABLE I. Exponents for the Gaussian basis functions used in the calculations. All Gaussian functions were uncontracted except the cases in parentheses. Here the contraction coefficients (for normalized primitives) were 0.020 528, 0.317 300, and 0.774 441 for Zn, and 0.576 412 9 and 0.518 9292 for Cd.

Symmetry	Cd	Hg	Zn	S	Se	Te	Po
S							6.0
S							1.9974
S	0.5095	0.5275	0.7997	1.85	1.033	0.6938	0.6658
S	0.1924	0.2334	0.17520	0.4035	0.6521	0.4038	0.3696
S	0.0544	0.06861	0.05560	0.1438	0.166	0.1165	0.1146
P							2.7
P	0.8270	0.6503	0.36	4.945	2.366	1.231	0.9172
P	0.1287	0.1368	0.1202	0.487	0.3833	0.2756	0.2671
P	0.0405	0.04256	0.0351	0.1379	0.1186	0.09108	0.0873
D	5.148	1.484	(68.85)				
D	(1.966)		(18.32)				
D			(5.922)				
D			1.927	0.487	0.3833	0.2756	0.2671
D	(0.7360)	0.5605	0.5528				
D	0.2479	0.1923	0.1202				

$$V_{e,pp}(\mathbf{r})=\int d\mathbf{r}_1\,\frac{[\rho_{pp}(\mathbf{r}_1)-\rho_{se}(\mathbf{r}_1)]}{|\mathbf{r}-\mathbf{r}_1|} \tag{15}$$

on the grid. Substituting (3) and (11) into (15) leads to

$$V_{e,pp}(\mathbf{r})=\sum_R\sum_a -\frac{Z_a}{|\mathbf{r}-\mathbf{R}-\mathbf{a}|}\left[\operatorname{erfc}(\sqrt{s_e}|\mathbf{r}-\mathbf{R}-\mathbf{a}|)-\sum_{i=1}^{2} C_i\operatorname{erfc}(\sqrt{\alpha_i}|\mathbf{r}-\mathbf{R}-\mathbf{a}|)\right]. \tag{16}$$

As $|\mathbf{r}-\mathbf{R}-\mathbf{a}|\to 0$, we obtain

$$V_{e,pp}(\mathbf{r})=-2\sum_R\sum_a Z_a\left[\sum_{i=1}^{2} C_i(\sqrt{\alpha_i/\pi}-\sqrt{s_e/\pi})\right], \tag{17}$$

so that there is no singularity.

This approach differs from the standard method[5(a)] of handling Ewald sums. The standard approach[5(a)] treats both electrons and pseudoions in the reciprocal space. Consequently the convergence in reciprocal space is strictly constrained by the softness of the pseudopotential. An alternative would be to use the reduced cell multipole method,[5(b)] which should improve the size scaling for large systems; however, the current systems are not large enough to require this.

The remaining term to evaluate is the term, E_{en}^{nl}, arising from the nonlocal PP. This requires evaluating three-center integrals over Gaussian functions, $\langle b|V_{pp,a}^{\mathrm{nl}}|c\rangle$. However, Hua, Chen, and Goddard[3] have shown that the nonlocal BHS PP can be replaced accurately by a separable PP of the form

$$V_{pp,a}^{\mathrm{sep}}=\sum_{n_a}|n_a\rangle\epsilon_{n_a}\langle n_a|, \tag{18}$$

where $|n_a\rangle$ are linear combinations of Gaussian functions centered on atom *a*. Thus the matrix elements become

$$\langle b|V_{\mathrm{nl}}^{a}|c\rangle=\sum_{n_a}\langle b|n_a\rangle\epsilon_{n_a}\langle n_a|c\rangle, \tag{19}$$

requiring only two-center matrix elements. These matrix elements are done easily using the recursion relations of Ref. 4.

III. BULK PROPERTIES OF II-VI SEMICONDUCTORS

To test the accuracy of using Gaussian basis functions for systems with periodic boundary conditions (PBC), we carried out GDSP/DFT calculations for 12 II-VI semiconductors, many of which are of current technological interest as infrared detectors and in optoelectronics.[6] As a starting point for constructing the basis sets, we used the primitive Gaussians in the Hay-Wadt (HW) basis sets.[7] Where these basis sets do not contain *d* polarization functions, we added polarization functions with exponents equal to the second outermost *p*-type basis function (generally within 10% of the optimum value). Where the HW basis sets contain more than three sets of *d* functions, contractions of the inner functions were used to reduce the number of independent functions to three. For CdTe crystal, the use of the contracted Cd basis leads to a total energy within 3×10^{-5} hartree of that using the uncontracted basis. Previous applications show this approach to be satisfactory.[1,3] The final basis sets used for the II-VI compounds are listed in Table I.

The calculations used the separable form of the BHS potential according to Ref. 3. The outer filled shell of *d* electrons on the cation plays a very important role in the II-VI semiconductors, as pointed out by Wei and Zunger[12] (see also discussions below), and we include explicitly these *d* electrons as valence electrons (thus Zn, Cd, Hg each have 12 electrons). We used the exchange-correlation potential of Ceperley-Alder as parametrized by Perdew and Zunger,[8] which is consistent with the pseudocore.[2] All band calculations used the ten special *k* points of Chadi and Cohen.[9] The results for the lattice constant and bulk modulus are summarized in Table II. Both GDSP/DFT and linear augmented

TABLE II. Properties for II-VI semiconductor crystals.

	ZnTe	CdTe	HgTe	ZnSe	CdSe	HgSe	ZnS	CdS	HgS	ZnPo	CdPo	HgPo
Lattice constant (Å)												
GDSP/DFT	6.020	6.430	6.530	5.591	6.035	6.194	5.302	5.804	5.975	6.201	6.624	6.666
Exper.	6.089[a]	6.48[a]	6.460[a]	5.669[a]	6.084[a]	6.074[a]	5.411[a]	5.83[a]	5.852[a]	6.309[b]	6.665[b]	
Others	6.052[c]	6.470[c]	6.492[c]	5.618[d]			5.345[d]	5.811[d]				
Bulk modulus (Mbar)												
GDSP/DFT	0.492	0.295	0.471	0.833	0.665	0.418	0.773	0.467	0.553	0.510	0.372	0.409
Exper.	0.509[b]	0.445[b]	0.476[b]	0.625[b]	0.550[b]	0.576[b]	0.769[b]	0.643[b]	0.686[b]			
Others	0.521[c]	0.440[c]	0.461[c]									

[a]Reference 10.
[b]Reference 11.
[c]Reference 12, scalar relativistic LAPW calculations.
[d]Reference 13, LAPW calculations.

plane-wave method (LAPW) underestimate slightly the lattice constant, except for the Hg compounds (where the lattice constant is slightly overestimated). This might be due to the errors in the local-density approximation (LDA).

The band structures were calculated at the theoretical lattice constant. The results on some high symmetry points are reported in Table III and in Fig. 1 (a group theoretic analysis of the band structures has not been done). Comparison of the band gap with experimental results and existing theoretical calculations are reported in Table IV. For a given anion, both experiment and theory show that the band gap decreases as the cations get heavier. As expected, the band gap in LDA calculations is too small. The exception is for mercury compounds where the inverted gaps are overestimated.

The inversion of the band gap in mercury compounds leads to metallic character. For Zn and Cd compounds the conduction-band minimum has $4s$ and $5s$ character while the dominant character at the valence-band maximum is anion balance p. However, the very large relativistic effects in mercury stabilize the $6s$ orbital significantly. This enhances the screening of the p and d bands, which has two effects. First, the anion p bands are pushed up. Second, the more weakly bound Hg d band enhances the Hg d-anion p band coupling, further pushing up the valence-band maximum. As a consequence of the strong p-d coupling, significant cation-d character is admixed to the valence-band maximum Γ_{15v} (10.4% for CdTe, 16.8% for HgTe, and 15.6% for HgPo). Thus, to understand the II-VI band structure one must account for both the cation-p–anion-p coupling and the cation-d–anion-p coupling.

Similarly, the polonium compounds are semimetals because relativistic effects push up the polonium p level (decreasing slightly the p-d coupling effects; see Table V). The relativistic effects are maximum for HgPo where the inverted gap is 1.89 eV.

Figure 2 illustrates the role of these couplings. Based on this scheme, it is possible to make a detailed analysis of the band structure using the band-consistent tight-binding model (BC-TB) as indicated in Sec. IV B.

IV. CALCULATIONS OF VALENCE-BAND OFFSETS

A. Band-consistent tight-binding (BC-TB) model

After calculating the band structure, it is useful to extract a simplified model for understanding the results or for com-

TABLE III. Energies (eV) at symmetry points from GDSP/DFT calculations (eV) for II-VI semiconductors.

	ZnTe	CdTe	HgTe	ZnSe	CdSe	HgSe	ZnS	CdS	HgS	ZnPo	CdPo	HgPo
Γ_{1v}	−12.02	−11.35	−11.74	−13.57	−12.76	−13.14	−13.51	−12.40	−12.78	−13.33	−12.67	−13.23
Γ_{15d}	−6.97	−8.22	−7.22	−6.60	−7.93	−6.91	−6.61	−7.70	−6.80	−7.11	−8.31	−7.30
Γ_{12d}	−6.67	−7.87	−6.69	−6.13	−7.43	−6.23	−5.98	−7.10	−5.98	−6.85	−8.01	−6.83
Γ_{15v}	0	0	0	0	0	0	0	0	0	0	0	0
Γ_{1c}	1.32	0.65	−0.84	1.39	0.45	−1.19	2.15	1.00	−0.69	−0.13	−0.44	−1.89
Γ_{15c}	4.38	4.54	4.22	6.01	5.80	5.41	6.49	6.57	6.09	4.17	4.32	4.05
X_{1v}	−10.70	−10.77	−11.03	−12.45	−12.23	−12.59	−12.05	−11.80	−12.16	−12.41	−12.24	−12.73
X_{3v}	−5.27	−4.51	−5.32	−4.87	−4.28	−4.92	−4.87	−4.11	−4.69	−5.30	−4.48	−5.43
X_{5v}	−2.31	−1.98	−2.20	−2.24	−1.98	−2.15	−2.46	−1.99	−2.16	−2.28	−1.92	−2.21
X_{1c}	2.12	2.43	2.43	3.05	2.94	2.93	3.18	3.42	3.35	1.92	2.43	2.04
X_{3c}	2.21	2.68	1.89	3.53	4.03	2.70	4.02	4.68	3.02	1.87	2.12	1.68
L_{1v}	−11.05	−10.91	−11.21	−12.74	−12.36	−12.73	−12.43	−11.94	−12.31	−12.66	−12.36	−12.87
L_{1v}	−5.49	−4.66	−5.38	−5.43	−4.65	−5.28	−5.75	−4.64	−5.25	−5.45	−4.58	−5.49
L_{3v}	−0.95	−0.82	−0.95	−0.87	−0.80	−0.9	−0.96	−0.79	−0.9	−0.95	−0.80	−0.96
L_{1c}	1.73	1.70	0.64	2.64	2.24	0.93	3.31	2.91	1.41	0.99	1.08	0.097

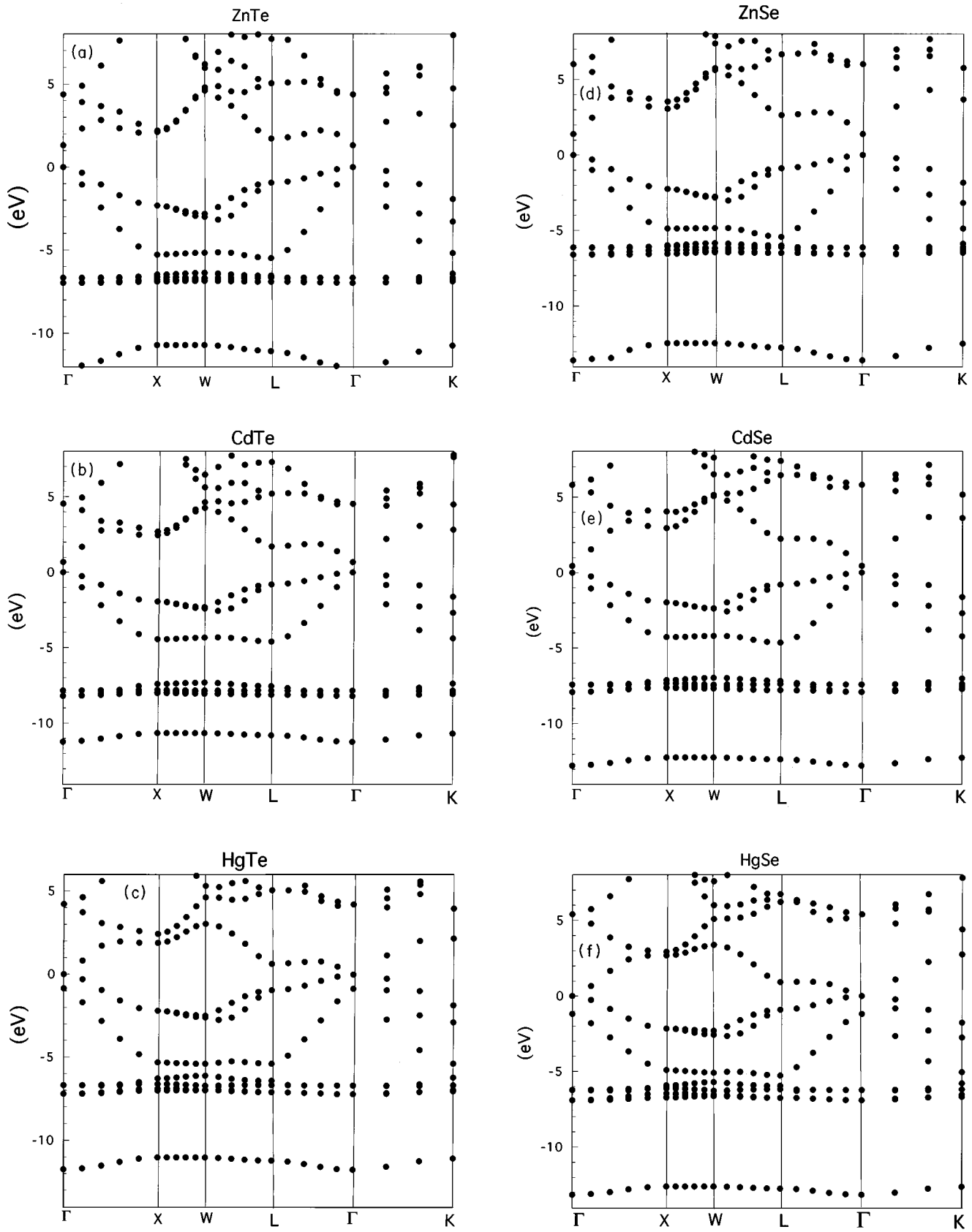

FIG. 1. Band structure along high symmetry directions for various II-VI semiconductors (calculated at theoretical equilibrium lattice constant). (a) ZnTe. (b) CdTe. (c) HgTe. (d) ZnSe. (e) CdSe. (f) HgSe. (g) ZnS. (h) CdS. (i) HgS. (j) ZnPo. (k) CdPo. (l) HgPo.

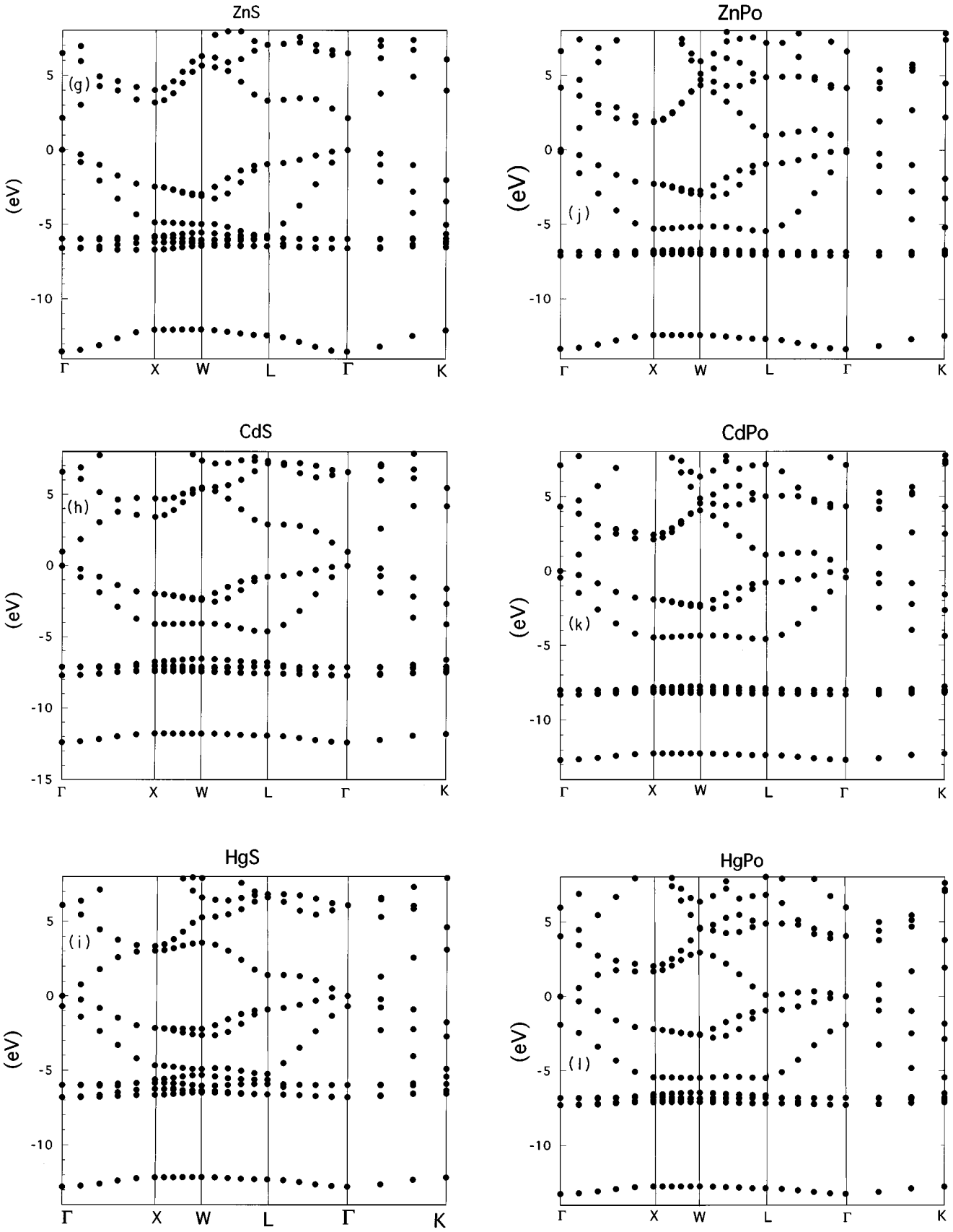

FIG. 1 (*Continued*).

TABLE IV. Band gaps (eV) from GDSP/DFT calculations.

	ZnTe	CdTe	HgTe	ZnSe	CdSe	HgSe	ZnS	CdS	HgS	ZnPo	CdPo	HgPo
GDSP/DFT	1.32	0.65	−0.84	1.39	0.45	−1.19	2.15	1.00	−0.69	−0.13	−0.44	−1.89
Exper.[a]	2.39	1.60	−0.3	2.87	1.82	−0.1	3.82	2.58	−0.2–0.5			
LAPW[b]	1.02	0.47	−0.99	1.6[c]			2.0[c]					

[a]Reference 14.
[b]Scalar relativistic LAPW calculations, Ref. 12.
[c]Estimated from Fig. 3 in Ref. 12. Calculations use nonrelativistic all-electron mixed-basis method.

paring systems. We describe here a simple tight-binding model that uses the self-consistent band structure to extract such parameters. A somewhat similar scheme was previously proposed by Wei and Zunger,[12] but our model does not require atomic information.

First we consider p-p coupling of anion and cation (left panel in Fig. 2). Simple two-band theory gives the splitting as

$$2\Delta_{pp}\equiv\Gamma_{15c}-\Gamma_{15v}(p)=2\sqrt{d_p^2+V_p^2}\,, \tag{20}$$

where $d_p\equiv(\epsilon_p^c-\epsilon_p^a)/2$ is half the distance between cation p and anion p levels and V_p is the coupling strength. The same argument leads to the distance between the bonding $\Gamma_{15v}(p)$ and the anion $p(t2)$ level (see Fig. 2)

$$d'=\sqrt{d_p^2+V_p^2}-d_p\,. \tag{21}$$

On the other hand, from second-order perturbation theory the fractional cation p charge is

$$q_p=\frac{(d'/V_p)^2}{1+(d'/V_p)^2}\,. \tag{22}$$

Defining

$$\gamma_p=\sqrt{(1-q_p)^{-1}-1)} \tag{23}$$

the above equations lead to

$$\frac{d_p}{V_p}=\frac{1-\gamma_p^2}{2\gamma_p}\,, \tag{24}$$

$$V_p=\frac{\Delta_{pp}}{\sqrt{1+(d_p/V_p)^2}}\,. \tag{25}$$

Now we turn to the p-d coupling (right panel in Fig. 2). If there were no p-d coupling, Δ_{pp} would be half of the distance $B\equiv\Gamma_{15c}-\Gamma_{15v}$. Because of the p-d coupling, B appears smaller by the amount of p-d shift, Δ_{pd}. Therefore, we have

$$\Delta_{pp}=\frac{B+\Delta_{pd}}{2}\,. \tag{26}$$

Again, two-band theory leads to

$$E_{pd}\equiv\Gamma_{15v}(pd)-\Gamma_{15d}(pd)=2\sqrt{[\epsilon_{15v}(p)-\epsilon_d]^2/4+V_{pd}^2}\,, \tag{27}$$

where $\epsilon_{15v}(p)$ would be the valence-band maximum if there were no p-d coupling, ϵ_d is the cation d level, and V_{pd} is the strength of p-d coupling. On the other hand, defining Δ_{pd} as the p-d shift, then it must be that

$$E_{pd}\equiv[\epsilon_{15v}(p)-\epsilon_d]+2\Delta_{pd}\,. \tag{28}$$

Thus (using second-order perturbation theory) the fractional charge of cation d charges in the $\Gamma_{15v}(pd)$ band is

$$q_d=\frac{(\Delta_{pd}/V_{pd})^2}{1+(\Delta_{pd}/V_{pd})^2}\,. \tag{29}$$

Defining $\gamma_d=\sqrt{(1-q_d)^{-1}-1}$, we have

TABLE V. Band-consistent tight-binding (BC-TB) analysis of the band structures for II-VI semiconductors at theoretical lattice constant.

	ZnTe	CdTe	HgTe	ZnSe	CdSe	HgSe	ZnS	CdS	HgS	ZnPo	CdPo	HgPo
B[a]	4.38	4.54	4.22	6.01	5.798	5.411	6.49	6.565	6.030	4.17	4.32	4.05
E_{pd}[b]	6.96	8.22	7.21	6.60	7.925	6.913	6.61	7.701	6.942	7.11	8.31	7.30
q_p[c]	0.05548	0.01713	0.02185	0.040391	0.01003	0.01240	0.01779	0.00696	0.00719	0.06741	0.02241	0.02719
Δ_{pp}[d]	2.6627	2.6965	2.7149	3.5941	3.4233	3.3951	3.8437	3.8738	3.759	2.5287	2.5383	2.5909
q_d[e]	0.1364	0.1041	0.1678	0.1782	0.1323	0.1995	0.1810	0.1536	0.2144	0.1244	0.0909	0.1555
Δ_{pd}[f]	0.9494	0.8559	1.2098	1.1753	1.0486	1.2949	1.1955	1.1826	1.4198	0.8844	0.7556	1.1347
$\delta\epsilon_d$[g]	0.31	0.35	0.53	0.46	0.49	0.68	0.63	0.60	0.82	0.26	0.30	0.47

[a]B is the distance between Γ_{15c} and Γ_{15v}.
[b]E_{pd} is the distance between the cation d level and the valence-band maximum.
[c]q_p is the cation p-type fractional charge.
[d]Δ_{pp} is the splitting due to the p-p coupling.
[e]q_d is the cation d-type fractional charge.
[f]Δ_{pd} is the splitting due to the p-d coupling.
[g]$\delta\epsilon_d$ is the cation d band width at the Γ point.

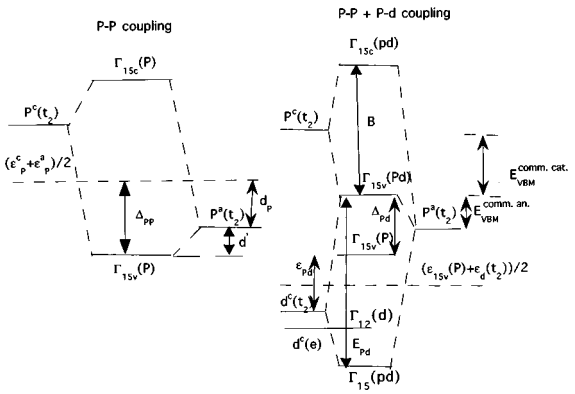

FIG. 2. Schematic picture of the band-consistent tight-binding (BC-TB) coupling mechanism in II-VI semiconductors.

$$V_{pd}=\frac{\gamma_d E_{pd}}{1+\gamma_d^2}\,, \tag{30}$$

$$\epsilon_{pd}\equiv\epsilon_{15v}(p)-\epsilon_d=\sqrt{E_{pd}^2-4V_{pd}^2}, \tag{31}$$

$$\Delta_{pd}=\frac{E_{pd}-\epsilon_{pd}}{2}\,. \tag{32}$$

It is important to emphasize that this theory uses no explicit atomic information, so that the result is band structure consistent. Table V gives the results from such analyses. With the same cation, the p-d splitting decreases as the anion gets heavier, correlating with the increase between cation d levels and anion p levels. For cases with common anions, Table V shows that the p-p splitting depends very little on the cations, correlating with the very similar lattice constants (and therefore similar p-p coupling strength) for these common anion materials. These observations suggest that the cation d electrons must be included in calculating such quantities as the band offset. In fact, aligning the bands on the anion p level, we obtain an excellent estimate of the band offsets for lattice-matched compounds having common anions. This occurs despite the neglect of screening effects due to the interface dipoles.

In the absence of p-d coupling, the valence-band maximum would be

$$E_{\mathrm{VBM}}^{(0)}-\epsilon_p^a=d_p-\Delta_{pp}\,. \tag{33}$$

Taking into account the p-d coupling, we have

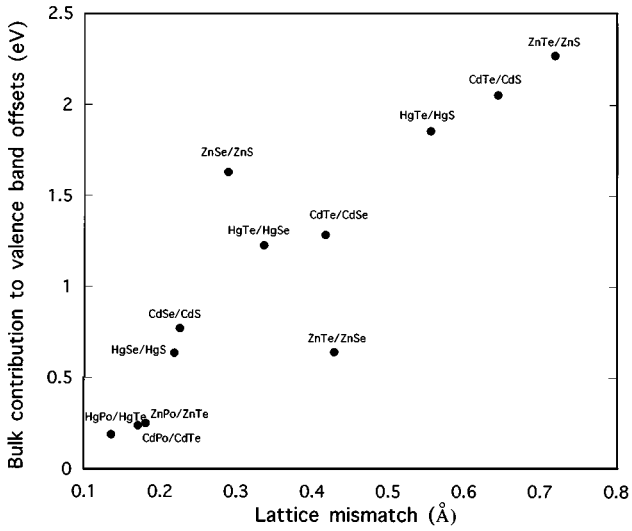

FIG. 3. Lattice-mismatch dependence of the bulk contribution to the valence-band offsets in common cation II-VI semiconductors. Because of the relatively larger lattice mismatches, p-p coupling is dominant in this class of superlattices and the lattice-mismatch dependence of the band offsets is close to linear. Note the compounds with lighter anion have smaller lattice constant and lower valence-band maxima (see text).

$$E_{\mathrm{VBM}}^{(1)}-\epsilon_p^a=d_p-\Delta_{pp}+\Delta_{pd}\,. \tag{34}$$

The resulting band offsets are reported in Table VI. The agreement with experimental data is very good for the lattice-matched CdTe/HgTe. The exception is for the ZnTe/HgTe superlattice (and therefore also CdTe/ZnTe because of transistivity). This has a larger lattice mismatch, making interface dipole screening effects and strain effects very important. The LAPW results of Ref. 17 are included in Table VI for comparison.

For compounds with common cations, the lattice mismatch is significantly larger (see Table II) and the interface dipole screening should become more important. Still, the bulk contributions provide useful information about the extent of interface effects. We report the bulk contribution to the valence-band offsets for these materials calculated using the current model (alignment on cation p levels) which neglects such screenings. Unfortunately, for these cases there are no experimental data to assess numerical accuracy. Comparison with available theoretical calculations is reasonably good (Table VII).

TABLE VI. Valence-band offsets for common anion II-VI semiconductors using the band-consistent tight-banding model (BC-TB). For comparison experimental data and available theoretical calculations are also reported. The results neglecting p-d coupling are also listed.

	CdTe HgTe	CdSE HgSe	CdS HgS	ZnTe CdTe	ZnSe CdSe	ZnS CdS	ZnTe HgTe	ZnSe HgSe	ZnS HgS	ZnPo CdPo	CdPo HgPo
BC-TB	−0.3137	−0.3156	−0.3019	−0.123	−0.094	−0.059	−0.436	−0.410	−0.361	−0.097	−0.353
No p-d	0.0217	0.0142	0.0126	−0.1977	−0.220	−0.081	−0.176	−0.171	−0.069	−0.227	0.027
Exper.	−0.35±0.006[a]			0.10±0.06[b]			−0.25±0.05[b]				
LAPW[c]	−0.377			0.125			−0.227				

[a]Reference 15, XPS experiment.
[b]Reference 16, XPS experiment.
[c]Reference 17, LAPW calculations.

TABLE VII. Valence-band offsets for common cation II-VI semiconductors using the band-consistent tight-binding model (BC-TB). There is no experimental data for comparison. Available theoretical calculations are also reported. The results neglecting p-d coupling (no pd) are listed.

	HgTe HgSe	HgTe HgS	HgSe HgS	CdTe CdSe	CdTe CdS	CdSe CdS	ZnTe AnSe	ZnTe ZnS	ZnSe ZnS	HgPo HgTe	CdPo CdTe	ZnPo ZnTe
BC-TB	1.2264	1.8568	0.6349	1.2849	2.0541	0.7692 (0.2192)	1.26	1.99	0.73	0.19	0.238	0.25
No pd	1.3957	2.1395	0.7438	1.4598	2.3532	0.8934 (0.3634)	1.48	2.24	0.75	0.27	0.358	0.31
Others						(0.23±0.1)[a]	1.20[b]		0.50∼0.25[c]			
							1.43[d]		0.10∼0.70[e]			
							0.86[f]					

[a]The data in parenthesis are for conduction-band offset. The experimental data (Ref. 18) are for Wurtzite form.
[b]Reference 21, model solid approximation.
[c]Reference 19, linear muffin-tin orbital (LMTO) supercell calculations.
[d]Reference 22, self-consistent tight binding.
[e]Reference 20, LMTO supercell calculations. The results depend strongly on strain modes and interfacial orientation.
[f]Reference 23, midgap theory.

We should emphasize that spin-orbit splittings of the valence bands are not included. Including spin-orbit effects would change the valence-band offset for CdTe/HgTe to ~ -0.3537, in very good agreement with experiment. (Our convention is that AB/CD is positive when the valence-band maximum of AB is higher than that of CD.)

The valence-band offsets of the three Cd-Hg common anion compounds are very similar. This is because the band offset is dominated by the differences of p-d coupling. The difference of the d bands for these materials is almost the same (-0.9 for CdTe/HgTe, -1.0 for CdSe/HgSe, and -0.92 for CdS/HgS) with very slightly larger band offset for CdSe/HgSe (corresponding to slightly larger d-band energy differences). Also, the Cd compounds have a consistently lower valence-band maximum (correlating with the fact that the Cd d band is lower) and therefore smaller p-d coupling. This is consistent with our calculations (see Δ_{pd} in Table V). Clearly, the shift of the valence-band maximum due to p-d

TABLE VIII. Theoretical calculations of bulk contributions and interface contributions to the valence-band offsets (eV). For CdTe/HgTe and CdTe/ZnTe, we use pseudopotentials (including d electrons) which include scalar relativistic effects. For GaN/AlN and GaAs/AlAs, all electrons are included. Calculations were done at the average theoretical lattice constant of the component compounds. Our convention is that AC/BC is positive when the valence band maximum of AC is higher than that of BC.

	CdTe/HgTe	CdTe/ZnTe	GaN/AlN	GaAs/AlAs
Bulk contributions				
BC-TB	−0.435	0.524	1.317	0.523
BC-TB (ignore p-d couplings)	0.030	−0.155	0.100	−0.046
GDS/DFT			1.189	0.682
Interface contributions				
GDS/DFT			−0.451	−0.199
Total valence-band offset				
GDS/DFT			0.738	0.493
Experiment	−0.35±0.06[a]	−0.10±0.06[b]	0.5[c]	0.4∼0.55[d]
Others	−0.377[e]	−0.125	0.85[f]	0.49∼0.51[g]

[a]Reference 15, XPS experiment.
[b]Reference 16, XPS experiment.
[c]Reference 28, photoluminescence.
[d]Reference 29.
[e]Reference 17, LAPW calculations.
[f]Reference 30, LMTO calculations.
[g]Reference 31, plane-wave pseudopotential calculations.

TABLE IX. Valence-band offsets (eV) measured from different core levels. The first index in parentheses refers to Ga core levels, while the second refers to Al core levels. Our convention is that AC/BC is positive when the valence-band maximum of AC is higher than that of BC.

	$(1s,1s)$	$(2s,1s)$	$(3s,1s)$	$(2s,2s)$	$(3s,2s)$	$(2p,2p)$	$(2p,3p)$
Bulk contributions							
GaAs/AlAs	0.493	0.417	0.420	0.397	0.400	0.392	0.395
GaN/AlN	0.738	0.782	0.755	0.698	0.671	0.695	0.702

coupling must be larger than the *d*-band width (see Fig. 1). This also is found in our calculations (Table V).

For superlattices with common cations, the compounds with the heavier anion always have a higher valence-band maximum. This directly correlates with the fact that heavier anions have shallower *p* levels (-5.74 for Po. -6.19 for Te, -6.74 for Se, and -7.19 for S) and significantly larger bond length. In these cases, *p*-*p* coupling dominates, resulting in a larger energy shift (downward with respect to cation *p* level) of the valence-band maxima in the lighter anion compounds. The larger differences in bond length lead to larger band offsets. From Table VII, we note that for common cation compounds, the bulk contribution to the valence-band offset is roughly proportional to the lattice mismatch (see Fig. 3).

B. Comparison with *ab initio* calculations of valence-band offset

In order to assess the accuracy of the BC-TB, we have calculated the valence-band offsets (VBO) of GaAs/AlAs and GaN/AlN using the all-electron GDS/DFT. The valence-band offset has two contributions, the bulk contribution and the interface contribution. The bulk contribution comes from the difference in ionization potential of the two bulk materials, while the interface contribution comes from the dipole screening of the offset due to charge transfer. Using all-electron calculations for common cation or common anion cases, the bulk contribution can be obtained by comparing the distance of the valence-band maxima (VBM) to the common core level, e.g., the As 1*s* level for GaAs/AlAs. This can be done with simple bulk calculations of the compounds. To include the effect of the interface, a superlattice calculation is necessary to obtain the difference of the core levels. Taking GaAs/AlAs as the example, one first calculates $\epsilon_l = E_{\mathrm{VBM}}^{\mathrm{GaAs}} - E_{\mathrm{core}}^{\mathrm{Ga}}$ and $\epsilon_r = E_{\mathrm{VBM}}^{\mathrm{AlAs}} - E_{\mathrm{core}}^{\mathrm{Al}}$ from bulk calculations. Then one calculates $d = E_{\mathrm{core}}^{\mathrm{Ga}} - E_{\mathrm{core}}^{\mathrm{Al}}$ from a GaAs/AlAs superlattice. The final VBO is given by $E_{\mathrm{VBO}} = \epsilon_l - \epsilon_r + d$. This procedure is valid only for lattice-matched cases. For lattice-mismatched heterojunctions, corrections to ϵ_l and ϵ_r are needed to account for the strain modification in the valence-band maximum.[27] The results for GaAs/AlAs and GaN/AlN are reported in Table VIII. The agreement with experiment is very good. Note the close agreement between ab initio results and BC-TB results for the bulk contributions to the valence-band offset. This provides quantitative support for the accuracy of BC-TB. To estimate the core-level shift, we report in Table IX the valence-band offset as measured from different core levels.

V. SUMMARY

We have implemented the dual space approach[1] for *ab initio* density functional calculations using Gaussian functions and separable pseudopotentials. This method takes the advantage of the locality of fields in real space, leading to the computational cost of Fock matrix (the most expensive part in a method using localized basis sets) scale linearly with the size of the basis set N for very large systems (it scales as $N^{3/2}$ for C_{60}).

There have been several other methods for electronic structure calculations using Gaussian basis set with pseudopotential approximations.[32,33] The current method has the advantage in that (1) a separate form of PP with general transferability is used; (2) the calculation of Coulomb potential is greatly accelerated using dual-space approach.[1]

We applied this GDSP/DFT method to studies of II-VI semiconductors. The bulk properties obtained are in very good agreement with existing experimental data and with LAPW calculations. We also applied GDSP/DFT to studies of II-VI surfaces and interfaces and to III-V interfaces.

We obtained valence-band offsets in excellent agreement with experiment and obtained unambiguous data on the bulk and interface contributions. A band-consistent tight-binding model is proposed that provides reasonably accurate estimates of the bulk contribution to the valence-band offset $E_{\mathrm{VBO}}^{\mathrm{bulk}}$. In the case of the lattice-matched common anion CdTe/HgTe, this is very close to the total VBO. The BC-TB model predicts that the $E_{\mathrm{VBO}}^{\mathrm{bulk}}$ scales linearly with the lattice mismatch for common cation cases. For lattice mismatched materials strain effects and interface contributions are important to the VBO. The purpose of the BC-TB calculation is to (1) assess quantitatively the importance of *d* electrons in II-VI systems by comparing the VBO obtained with and without *p*-*d* coupling and (2) obtain physical insight into how the heterojunction VBO depends on the component bulk electronic structure. The results presented here clearly demonstrate the importance of *d* electrons in the VBO of II-VI systems. They also provide a systematic understanding of the bulk contribution to the heterojunction VBO in terms of the electronic properties of the component semiconductors.

ACKNOWLEDGMENTS

This work was partially funded by the NSF (ASC 92-100368). Part of the computations were carried on the JPL Cray-YMP under the Caltech-JPL supercomputing project and on Cray-YMP at the Goddard Space Center. The facilities of the MSC is also supported by grants from DOE-BCTR, Asahi Chemical, Asahi Glass, Chevron Petroleum Technology, BF Goodrich, Xerox, Hughes Research Lab, Hercules, Teijin Ltd., and Beckman Institute.

*Present address: Schrödinger Inc., 80 S. Lake Ave. (Suite 735), Pasadena, California 91101.
†Author to whom correspondence should be addressed.

[1] X. J. Chen, J.-M. Langlois, and W. A. Goddard III, Phys. Rev. B **52**, 2348 (1995); Xiaojie Chen, Abner Mintz, Jinsong Hu, Xinlei Hua, Jenna Zinck, and William A. Goddard III, J. Vac. Sci. Technol. B **13**, 1715 (1995).
[2] G. B. Bachelet, D. R. Hamann, and M. Schlüter, Phys. Rev. B **26**, 4199 (1982).
[3] X. Hua, X. J. Chen, and W. A. Goddard III (unpublished).
[4] S. Obara and A. Saika, J. Chem. Phys. **84**, 3963 (1986).
[5] (a) J. Ihm, A. Zunger, and M. L. Cohen, J. Phys. C **12**, 4409 (1979); (b) H. Q. Ding, N. Karasawa, and W. A. Goddard, J. Chem. Phys. **97**, 4309 (1992); Chem. Phys. Lett. **196**, 6 (1992).
[6] See, for example, D. B. Eason, Z. Yu, W. C. Hughes, C. Boney, J. W. Cook, Jr., and J. F. Schetzina, J. Vac. Sci. Technol. B **13**, 1566 (1995); J. M. Arias, M. Zandian, R. Zucca, and R. E. DeWames, Appl. Phys. Lett. **58**, 2806 (1991).
[7] P. J. Hay and W. R. Wadt, J. Chem. Phys. **82**, 270 (1985).
[8] D. M. Ceperley and B. I. Alder, Phys. Rev. Lett. **45**, 566 (1980); J. P. Perdew and A. Zunger, Phys. Rev. B **23**, 5048 (1981).
[9] D. J. Chadi and M. L. Cohen, Phys. Rev. B **8**, 5747 (1973).
[10] N. Kh. Abrikosov, V. B. Bankina, L. V. Poretskaya, L. E. Shelimova, and E. V. Skudnova, *Semiconducting II-VI, IV-VI, and V-VI Compounds* (Plenum, New York 1969), p. 2.
[11] *Semiconductors, Physics of II-VI and I-VII Compounds, Semimagnetic Semiconductors*, edited by O. Madelung, Landolt-Börnstein, New Series, Group III, Vol. 17, Pt. a (Springer-Verlag, Berlin, 1982).
[12] S. H. Wei and Alex Zunger, Phys. Rev. B **37**, 8958 (1988).
[13] C.-Y. Yeh, W. Lu, S. Froyen, and A. Zunger, Phys. Rev. B **46**, 10 086 (1992).
[14] W. H. Strehlow and E. L. Cook, J. Phys. Chem. Ref. Data **2**, 163 (1973).
[15] S. P. Kowalczyk, J. T. Cheung, E. A. Kraut, and R. W. Grant, Phys. Rev. Lett. **56**, 1605 (1986).
[16] T. M. Duc, C. Hsu, and J. P. Faurie, Phys. Rev. Lett. **58**, 1127 (1987).
[17] S. H. Wei and A. Zunger, Phys. Rev. Lett. **59**, 144 (1987).
[18] M. P. Halsall, J. E. Nicholls, J. J. Davies, B. Cockayne, and P. J. Wright, J. Appl. Phys. **71**, 907 (1992).
[19] M. Methfessel and M. Scheffler, Physica (Amsterdam) B **172**, 175 (1991).
[20] N. E. Christensen and I. Gorczyca, Phys. Rev. B **44**, 1707 (1991).
[21] K. Shahzad, D. J. Olego, and C. H. van der Walle, Phys. Rev. B **38**, 1417 (1988).
[22] C. Priester, D. Bertho, and C. Jouanin, Physica (Amsterdam) B **191**, 1 (1993).
[23] J. Tersoff, Phys. Rev. Lett. **56**, 2755 (1986).
[24] For ZnSe/Ge, N. E. Christiansen [Phys. Rev. B **37**, 4528 (1988)] gives 1.393 V, while C. G. van der Walle *et al.* [J. Vac. Sci. Technol. B **4**, 1055 (1986)] gives 2.17 eV.
[25] R. B. Ross, J. M. Powers, T. Atashroo, W. C. Ermler, L. A. LaJohn, and P. A. Christiansen, J. Chem. Phys. **93**, 6654 (1990).
[26] R. C. Weast, *Handbook of Chemistry and Physics*, 74th ed. (CRC, Boca Raton, 1993–1994), p. 12–79.
[27] Chris G. Van de Walle and Richard Martin, Phys. Rev. B **34**, 5621 (1986).
[28] J. Bauer *et al.*, Appl. Phys. Lett. **65**, 2211 (1994).
[29] W. I. Wang *et al.*, Phys. Rev. B **3**, 1280 (1985), and references therein.
[30] E. A. Albanesi *et al.*, J. Vac. Sci. Technol. B **12**, 2470 (1994).
[31] A. Baldereschi *et al.*, Phys. Rev. Lett. **61**, 734 (1988).
[32] J. R. Chelikowsky, S. G. Louie, Phys. Rev. B **29**, 3470 (1984).
[33] B. N. Harmon, W. Weber, and D. R. Hamann, Phys. Rev. B **25**, 1109 (1982).